Vol 453|1 May 2008|doi:10.1038/nature06829

LETTERS

Melanopsin cells are the principal conduits for rod–cone input to non-image-forming vision

Ali D. Güler[1]*, Jennifer L. Ecker[1]*, Gurprit S. Lall[2]*, Shafiqul Haq[3], Cara M. Altimus[1], Hsi-Wen Liao[3], Alun R. Barnard[2], Hugh Cahill[3], Tudor C. Badea[4], Haiqing Zhao[1], Mark W. Hankins[5], David M. Berson[6], Robert J. Lucas[2], King-Wai Yau[3] & Samer Hattar[1]

Rod and cone photoreceptors detect light and relay this information through a multisynaptic pathway to the brain by means of retinal ganglion cells (RGCs)[1]. These retinal outputs support not only pattern vision but also non-image-forming (NIF) functions, which include circadian photoentrainment and pupillary light reflex (PLR). In mammals, NIF functions are mediated by rods, cones and the melanopsin-containing intrinsically photosensitive retinal ganglion cells (ipRGCs)[2,3]. Rod–cone photoreceptors and ipRGCs are complementary in signalling light intensity for NIF functions[4–12]. The ipRGCs, in addition to being directly photosensitive, also receive synaptic input from rod–cone networks[13,14]. To determine how the ipRGCs relay rod–cone light information for both image-forming and non-image-forming functions, we genetically ablated ipRGCs in mice. Here we show that animals lacking ipRGCs retain pattern vision but have deficits in both PLR and circadian photoentrainment that are more extensive than those observed in melanopsin knockouts[8,10,11]. The defects in PLR and photoentrainment resemble those observed in animals that lack phototransduction in all three photoreceptor classes[6]. These results indicate that light signals for irradiance detection are dissociated from pattern vision at the retinal ganglion cell level, and animals that cannot detect light for NIF functions are still capable of image formation.

The retinal ganglion cells that express melanopsin (rendering them intrinsically photosensitive) send monosynaptic projections to the suprachiasmatic nucleus (SCN) and the intergeniculate leaflet (IGL), responsible for circadian photoentrainment, and the olivary pretectal nucleus (OPN), responsible for PLR[15]. It has been reported that RGCs that do not contain melanopsin innervate the same NIF brain centres[15–19]. In mice genetically engineered to lack melanopsin protein, the RGCs that would normally express this opsin still project to the NIF centres, but these cells are no longer intrinsically photosensitive[8]. In these animals, PLR and circadian light responses are reduced but not absent, indicating that rods and cones are capable of light detection for NIF functions[8–11]. The rod–cone signals for NIF functions are undoubtedly relayed to the brain by RGCs, but it is unclear whether ipRGCs, conventional RGCs, or both are responsible (Fig. 1a).

To eliminate ipRGCs, we introduced a gene (*aDTA*) encoding attenuated diphtheria toxin A subunit (aDTA)[20] into the mouse gene locus encoding melanopsin (Supplementary Fig. 1a, b). Using antibody staining in retinas from animals expressing *aDTA* ($Opn4^{aDTA/+}$), we found that 3.1 ± 1.5% (mean ± s.e.m.) of melanopsin cells remained in the $Opn4^{aDTA/+}$ animals (Fig. 1b). Staining with 5-bromo-4-chloro-3-indolyl-β-D-galactoside (X-gal) in animals with the *aDTA* gene in one melanopsin allele and *tau-LacZ* in the other ($Opn4^{aDTA/tau\text{-}LacZ}$)[3] revealed that 17.2 ± 1.0% of melanopsin cells remained in the retinas of these animals at six months of age (Fig. 1c). Consistent with the elimination of ipRGCs, we observed fewer fibre terminals in the SCN, IGL and OPN of $Opn4^{aDTA/tau\text{-}LacZ}$ animals than in those of $Opn4^{tau\text{-}LacZ/+}$ animals (Fig. 2a–c). The degree of ipRGC ablation in the heterozygous animals increased with age (Supplementary Fig. 2a–c).

To ablate ipRGCs more completely, we generated animals homozygous for *aDTA* ($Opn4^{aDTA/aDTA}$). The morphology and thickness of the retina in the $Opn4^{aDTA/aDTA}$ animals were not different from those in wild types (Fig. 1d). Injection of fluorescently conjugated cholera toxin into the eye, which labels all ganglion cell fibres from the retina, showed that few fibres innervated the SCN and IGL in the $Opn4^{aDTA/aDTA}$ animals (Fig. 2d, e). Furthermore, comparison between age-matched $Opn4^{aDTA/+}$ and $Opn4^{aDTA/aDTA}$ mice verified that the extent of ipRGC ablation was greater in homozygous animals (Supplementary Fig. 2d). We also observed that target innervation by other RGCs was unaffected both in the dorsal lateral geniculate nucleus, which is important for image formation, and in the rostral core of the OPN[15] (Fig. 2e, f).

To assess whether image-forming functions are affected in animals expressing aDTA, we measured electroretinograms, optokinetic nystagmus responses, visual acuity and the ability of the animals to detect a visual cue. We found that the electroretinograms and optokinetic nystagmus responses were normal in animals lacking ipRGCs (Supplementary Fig. 3a, b). On the basis of optomotor responses, the acuity of $Opn4^{aDTA/aDTA}$ mice was slightly decreased compared with that of the wild-type mice (Fig. 1e) and $Opn4^{tau\text{-}LacZ/tau\text{-}LacZ}$ mice (Supplementary Fig. 3d). This effect is most probably due to enlarged pupil diameters in the $Opn4^{aDTA/aDTA}$ animals (see Fig. 3c and Supplementary Fig. 3c). We also determined that these animals could use a visual cue to locate a flag-marked platform in a water maze (Fig. 1e). These results demonstrate that image formation is functional despite the elimination of ipRGCs in $Opn4^{aDTA/aDTA}$ animals. We could therefore determine the relative contribution of ipRGCs to PLR and circadian photoentrainment in the context of normal image formation.

Pupil constriction regulates the amount of light entering the eye, and thus pupil diameter is negatively correlated with light intensity. At high light intensity, the iris decreases the area of the pupil by 95% (full constriction) in comparison with dark-adapted conditions (fully dilated). At low light intensity in which the pupil constricts

[1]Department of Biology, Johns Hopkins University, Baltimore, Maryland 21218, USA. [2]Faculty of Life Sciences, University of Manchester, Manchester M13 9PT, UK. [3]Department of Neuroscience, and [4]Molecular Biology and Genetics, Johns Hopkins University School of Medicine, Baltimore, Maryland 21205, USA. [5]Visual Neuroscience, University of Oxford, Oxford OX3 7BN, UK. [6]Department of Neuroscience, Brown University, Providence, Rhode Island 02912, USA.
*These authors contributed equally to this work.

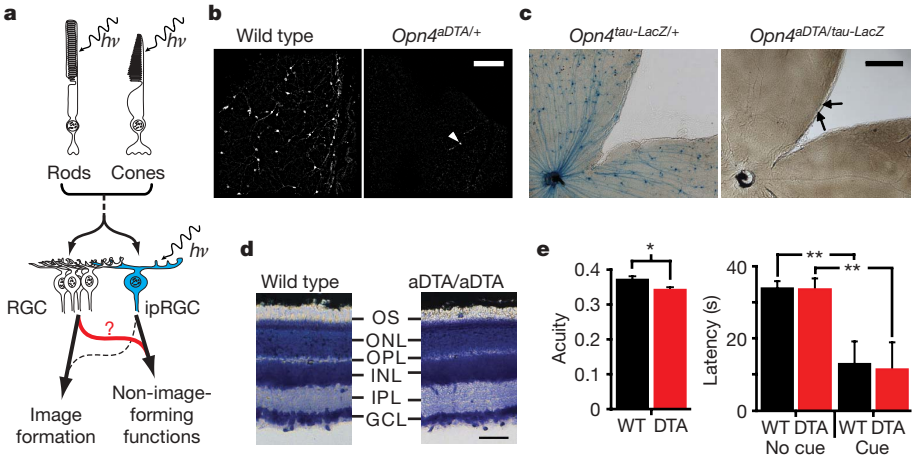

Figure 1 | Elimination of ipRGCs in mouse retina. **a**, Model describing how rod–cone signalling through conventional RGCs or ipRGCs contributes to NIF functions. The role of ipRGCs in image formation is speculative (dotted line). **b**, Melanopsin antibody staining in retinas of 18-month-old wild-type ($n = 6$) and $Opn4^{aDTA/+}$ ($n = 12$) mice. The white arrowhead indicates a surviving ipRGC. Scale bar, 200 μm. **c**, X-gal staining from $Opn4^{tau\text{-}LacZ/+}$ ($n = 6$) and $Opn4^{aDTA/tau\text{-}LacZ}$ ($n = 8$). The surviving cells are weakly stained (black arrows). Scale bar, 500 μm. **d**, Cross-sections of Giemsa-stained retinas from 18-month-old $Opn4^{aDTA/aDTA}$ (aDTA/aDTA; $n = 3$) and wild-type ($n = 3$) mice. The morphology of retinas is indistinguishable between genotypes. GCL, ganglion cell layer; IPL, inner plexiform layer; INL, inner nuclear layer; OPL, outer plexiform layer; ONL, outer nuclear layer; OS, outer segment. Scale bar, 50 μm. **e**, Left, the acuity (in cycles per degree) of $Opn4^{aDTA/aDTA}$ mice (DTA; $n = 11$; red bar) was slightly decreased in comparison with wild-type mice (WT; $n = 9$; black bar). Right, the latency to locate a marked platform (cue) in a water maze was similar in $Opn4^{aDTA/aDTA}$ (DTA; $n = 14$; red bar) and wild-type (WT; $n = 12$; black bar) mice. This latency significantly differed from that for unmarked platform (no cue) tests. All statistical comparisons used Student's *t*-test (asterisk, $P < 0.05$; two asterisks, $P < 0.01$); error bars indicate s.e.m.

by 50% or less, rod–cone input is the main signal[8,12] (Supplementary Table 1). In contrast, the intrinsic photosensitivity through the melanopsin protein in ipRGCs is necessary for full pupil constriction[8,12] (Supplementary Table 1). We found that the PLR was absent in all $Opn4^{aDTA/+}$ mice at a light intensity that constricts the pupil in wild-type animals to about 50% (Fig. 3a, b). This result suggests that although the melanopsin protein is not required for PLR at low light intensity, rod–cone input still requires the ipRGCs. We propose that ipRGCs are able to encode light intensities that are below the detection level of the melanopsin photopigment by integrating rod–cone signals and relaying this information to the OPN for pupil constriction.

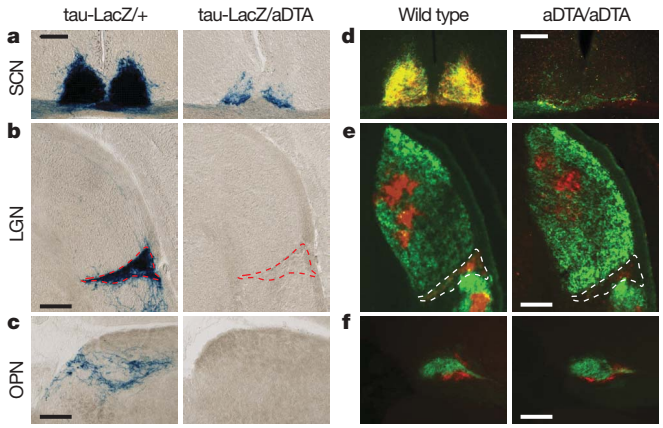

Figure 2 | The ipRGC fibres in the brain decrease in *aDTA* mice. **a**–**c**, X-gal staining in $Opn4^{tau\text{-}LacZ/aDTA}$ mice (tau-LacZ/aDTA; $n = 2$) shows that ipRGC innervation of the SCN, IGL and OPN is decreased in comparison with $Opn4^{tau\text{-}LacZ/+}$ mice (tau-LacZ/+; $n = 2$). **d**–**f**, Ocular cholera toxin injections (left eye, green; right, red) of $Opn4^{aDTA/aDTA}$ mice (aDTA/aDTA; $n = 11$) and wild-type mice ($n = 6$). **a**, **d**, SCN innervation is sparse in *aDTA* mice. **b**, **e**, The dorsal lateral geniculate nucleus (LGN) is innervated similarly both in *aDTA* and wild-type animals, whereas few fibres remain in the IGL of mutant mice (outlined regions). **c**, **f**, The OPN shell is innervated by ipRGCs and the core is targeted by other RGCs[15]. **c**, Fibres in the shell region are eliminated in $Opn4^{tau\text{-}LacZ/aDTA}$ animals. **f**, Fibres in the OPN core are retained in $Opn4^{aDTA/aDTA}$ mice. Scale bars, 200 μm.

At high light intensity, six of nine $Opn4^{aDTA/+}$ mice constricted their pupils to 95%, in a similar manner to wild-type animals (Fig. 3a, b). Full pupil constriction in these six animals indicates that the intrinsic photosensitivity persists in the remaining ipRGCs in $Opn4^{aDTA/+}$ mice and that only about 17% of ipRGCs are sufficient to drive full pupil constriction. The remaining three animals had

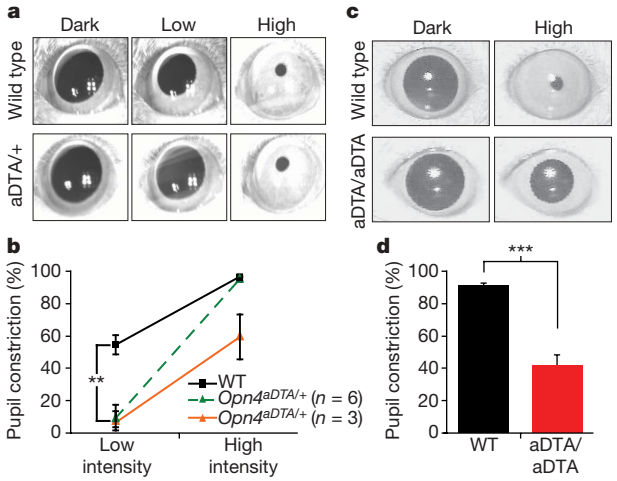

Figure 3 | *Opn4*^{aDTA} mice have deficits in PLR. **a**, All nine $Opn4^{aDTA/+}$ (aDTA/+) mice showed defective PLR at a light intensity (1.8 μW cm^{-2}; 30 s white light; Low) that induced 50% constriction in wild types. The $Opn4^{aDTA/+}$ mice showed a 9.0 ± 6.0% constriction. Six of nine $Opn4^{aDTA/+}$ mice had full pupil constriction at high light intensity (3 mW cm^{-2}; High). The rest of the mutant mice (three of nine) showed defective PLR. **b**, Quantification of PLR data of wild-type (WT; $n = 9$; black squares) and $Opn4^{aDTA/+}$ either photoentrained (green triangles; $n = 6$) or non-photoentrained (orange triangles; $n = 3$) animals. All statistical comparisons were made by Student's *t*-test (two asterisks, $P < 0.01$). **c**, All $Opn4^{aDTA/aDTA}$ animals (aDTA/aDTA) constrict their pupils only to a maximum of 42% after a light pulse that causes 95% constriction in wild types (161 μW cm^{-2}, 470 nm monochromatic light; High). **d**, Quantification of PLR data of wild-type (WT; $n = 11$; black bar) and $Opn4^{aDTA/aDTA}$ ($n = 12$; red bar) mice from **c**. Statistical comparisons were made by Student's *t*-test (three asterisks, $P < 0.001$); error bars indicate s.e.m.

pupil constriction defects at high light intensity (59 ± 14%, in contrast with 96 ± 1% in the wild type; Fig. 3b). Interestingly, when the $Opn4^{aDTA/+}$ animals were placed under 24-h light/dark cycles, animals that had full pupil constriction photoentrained (Supplementary Fig. 4a), whereas animals with defective pupil constriction had photoentrainment defects (Supplementary Fig. 4b).

The *aDTA* homozygotes have greater ablation of ipRGCs, and consequently all 12 $Opn4^{aDTA/aDTA}$ animals had defective PLR (42 ± 6%) at high light intensity (Fig. 3c, d). A similar pupil constriction (about 40%) to that observed in $Opn4^{aDTA/aDTA}$ mice is achieved by both wild-type and melanopsin knockout animals in response to a light stimulation that is about 1,000-fold lower in intensity[8]. This reduction in pupil sensitivity was observed in an intensity–response curve in $Opn4^{aDTA/aDTA}$ mice at constrictions that are 55% or higher in the wild types (Supplementary Fig. 5). Together, these data show that the rod–cone-dependent pupil constriction is reliant on signalling through ipRGCs at all light intensities (Fig. 3 and Supplementary Fig. 5). The residual pupil constriction observed in the homozygous animals may reveal a possible role for the non-melanopsin RGCs in pupil constriction. Alternatively, this residual pupil constriction could originate from rod–cone input through a few remaining ipRGCs in the $Opn4^{aDTA/aDTA}$ mice.

To assess the contribution of ipRGCs to circadian photoentrainment, we analysed the wheel running activity of wild-type ($n = 11$) and $Opn4^{aDTA/aDTA}$ ($n = 12$) animals using 24-h light/dark cycles. Under constant dark conditions (DD), both wild-type and $Opn4^{aDTA/aDTA}$ animals had a functional circadian oscillator with period lengths of 23.3 ± 0.1 and 23.8 ± 0.1 h, respectively (Fig. 4a). In a similar manner to $math5^{-/-}$ mice with severe optic nerve hypoplasia due to RGC loss, $Opn4^{aDTA/aDTA}$ animals had significantly longer periods than wild types (Supplementary Table 2), confirming the loss of the fibres projecting to the SCN[21]. A light stimulus (1,500 lx) administered for 15 min at circadian time (CT)16 delayed the phase onset of the activity of the wild types by 1.66 ± 0.23 h, whereas it did not affect the phase onset of activity in any $Opn4^{aDTA/aDTA}$ animals (−0.06 ± 0.09 h) (Fig. 4a). When the light/dark cycle was advanced or delayed by 6 h, the activity of all wild-type animals synchronized with the shifted cycle (Fig. 4b and Supplementary Table 2). $Opn4^{aDTA/aDTA}$ animals segregated into two groups with distinct responses. The first group of animals (8 of 12) free-ran completely under the shifted light/dark cycle (Fig. 4b and Supplementary Fig. 6b–f) in a similar manner to animals lacking all functional photoreceptors in the retina[6], indicating that they were completely blind to the light shift. Animals in the second group (4 of 12) were weakly light responsive but not photoentrained, because they did not show a stable phase relation to the light/dark cycle (Supplementary Fig. 7). Given that these four animals demonstrated very weak light responsiveness in the light/dark cycle but were not phase-shifted by the 15-min light pulse, we tested whether constant light (LL) conditions would lengthen the circadian period of $Opn4^{aDTA/aDTA}$ mice. Under LL, 7 of 11 wild-type animals had periods longer than 24 h, whereas the remaining animals became

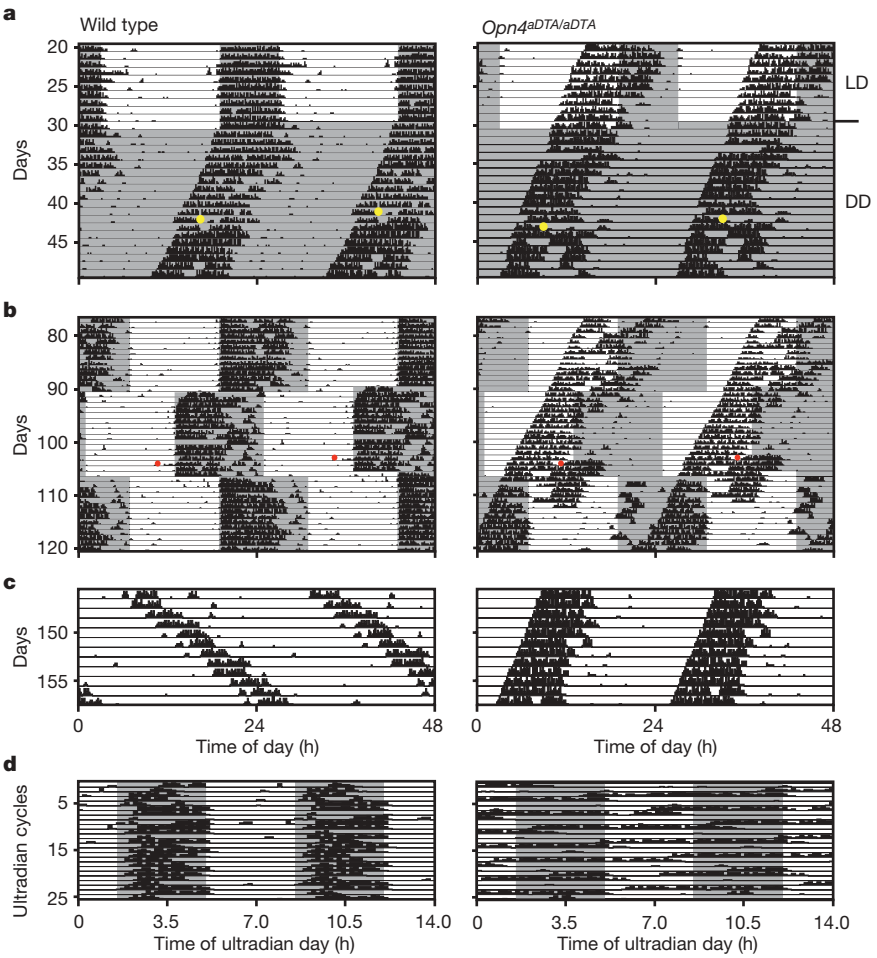

Figure 4 | $Opn4^{aDTA/aDTA}$ mice do not photoentrain or mask. **a**, $Opn4^{aDTA/aDTA}$ mice free-run under light/dark cycles (grey and white backgrounds; dark and light (about 700 lx), respectively). $Opn4^{aDTA/aDTA}$ mice do not phase shift in response to a 15-min 1,500-lx pulse of white light (CT16; yellow dots indicate light pulses). **b**, $Opn4^{aDTA/aDTA}$ mice do not photoentrain to the 24-h light/dark cycle in the delay or advance phases (red dots indicate cage changes). **c**, Unlike wild-type animals, no $Opn4^{aDTA/aDTA}$ mice lengthened their period under constant light. **d**, $Opn4^{aDTA/aDTA}$ mice do not mask under a 7-h ultradian cycle.

completely arrhythmic (Supplementary Fig. 6a). In contrast, both groups of *Opn4*$^{aDTA/aDTA}$ animals had periods shorter than 24 h (Fig. 4c, Supplementary Figs 6b–f and 7, and Supplementary Table 2). It had previously been shown that animals lacking only the melanopsin protein are similar to wild-type controls in adjusting to a 24-h light/dark cycle and have minor defects in their period lengthening under constant light and phase-delaying pulses of light[10,11]. The severe defects in circadian photoentrainment observed in animals lacking ipRGCs demonstrate that these cells are required not only for intrinsically signalling light information through the melanopsin protein but also for conveying rod–cone light information to the SCN. Although several reports indicated that RGCs that do not express melanopsin innervate the SCN[17–19,22], our results reveal that the contribution of rod–cone signalling through these RGCs for photoentrainment is negligible.

The acute effects of light on activity (also known as masking) can be studied by using an ultradian 7-h light/dark (3.5:3.5 LD) cycle that disrupts the oscillator[6]. Under the ultradian regime, wild types confined their activity mostly to the dark portion of the ultradian cycle ($84 \pm 4\%$). In contrast, the *Opn4*$^{aDTA/aDTA}$ animals were active nearly randomly across an ultradian day, irrespective of light ($64 \pm 3\%$; Fig. 4d). This result demonstrates that melanopsin cells are essential for a direct light-driven physiological response that is independent of the circadian oscillator.

We have shown that the loss of ipRGCs does not influence image formation and therefore the involvement of this ganglion cell class in classical vision is only modulatory[13,23]. In contrast, irradiance-dependent NIF functions are substantially impaired in the absence of ipRGCs. Given that the ipRGCs constitute less than 2% of the total RGC population, it is striking that light information for circadian photoentrainment and PLR is conveyed predominantly through these cells. Moreover, the ability to form pattern vision does not affect photoentrainment.

METHODS SUMMARY

Animals. All experiments were conducted in accordance with National Institutes of Health guidelines and were approved by institutional animal care and use committees of the universities involved.

Behavioural analyses. We used behavioural tests measuring the integrity of the outer retina (electroretinograms)[23], eye-tracking functions (optokinetic nystagmus)[24], visual acuity (optomotor)[25], object identification (water maze)[26], pupil constriction (PLR)[8,12], the period of the circadian oscillator (wheel running activity)[10,11], the adjustment of the circadian clock to different light stimulations (circadian photoentrainment, phase shifting, and constant light)[10,11] and direct light effects on activity (masking)[9].

Full Methods and any associated references are available in the online version of the paper at www.nature.com/nature.

Received 11 July 2007; accepted 7 February 2008.
Published online 23 April 2008.

1. Hubel, D. H. *Eye, Brain, and Vision* (Freeman, New York, 1988).
2. Berson, D. M., Dunn, F. A. & Takao, M. Phototransduction by retinal ganglion cells that set the circadian clock. *Science* **295,** 1070–1073 (2002).
3. Hattar, S., Liao, H. W., Takao, M., Berson, D. M. & Yau, K. W. Melanopsin-containing retinal ganglion cells: architecture, projections, and intrinsic photosensitivity. *Science* **295,** 1065–1070 (2002).
4. Freedman, M. S. *et al.* Regulation of mammalian circadian behavior by non-rod, non-cone, ocular photoreceptors. *Science* **284,** 502–504 (1999).
5. Czeisler, C. A. *et al.* Suppression of melatonin secretion in some blind patients by exposure to bright light. *N. Engl. J. Med.* **332,** 6–11 (1995).
6. Hattar, S. *et al.* Melanopsin and rod–cone photoreceptive systems account for all major accessory visual functions in mice. *Nature* **424,** 75–81 (2003).
7. Panda, S. *et al.* Melanopsin is required for non-image-forming photic responses in blind mice. *Science* **301,** 525–527 (2003).
8. Lucas, R. J. *et al.* Diminished pupillary light reflex at high irradiances in melanopsin-knockout mice. *Science* **299,** 245–247 (2003).
9. Mrosovsky, N. & Hattar, S. Impaired masking responses to light in melanopsin-knockout mice. *Chronobiol. Int.* **20,** 989–999 (2003).
10. Panda, S. *et al.* Melanopsin (*Opn4*) requirement for normal light-induced circadian phase shifting. *Science* **298,** 2213–2216 (2002).
11. Ruby, N. F. *et al.* Role of melanopsin in circadian responses to light. *Science* **298,** 2211–2213 (2002).
12. Lucas, R. J., Douglas, R. H. & Foster, R. G. Characterization of an ocular photopigment capable of driving pupillary constriction in mice. *Nature Neurosci.* **4,** 621–626 (2001).
13. Dacey, D. M. *et al.* Melanopsin-expressing ganglion cells in primate retina signal colour and irradiance and project to the LGN. *Nature* **433,** 749–754 (2005).
14. Wong, K. Y., Dunn, F. A., Graham, D. M. & Berson, D. M. Synaptic influences on rat ganglion-cell photoreceptors. *J. Physiol. (Lond.)* **582,** 279–296 (2007).
15. Hattar, S. *et al.* Central projections of melanopsin-expressing retinal ganglion cells in the mouse. *J. Comp. Neurol.* **497,** 326–349 (2006).
16. Gooley, J. J., Lu, J., Fischer, D. & Saper, C. B. A broad role for melanopsin in nonvisual photoreception. *J. Neurosci.* **23,** 7093–7106 (2003).
17. Hannibal, J. & Fahrenkrug, J. Target areas innervated by PACAP-immunoreactive retinal ganglion cells. *Cell Tissue Res.* **316,** 99–113 (2004).
18. Morin, L. P., Blanchard, J. H. & Provencio, I. Retinal ganglion cell projections to the hamster suprachiasmatic nucleus, intergeniculate leaflet, and visual midbrain: bifurcation and melanopsin immunoreactivity. *J. Comp. Neurol.* **465,** 401–416 (2003).
19. Sollars, P. J. *et al.* Melanopsin and non-melanopsin expressing retinal ganglion cells innervate the hypothalamic suprachiasmatic nucleus. *Vis. Neurosci.* **20,** 601–610 (2003).
20. Maxwell, F., Maxwell, I. H. & Glode, L. M. Cloning, sequence determination, and expression in transfected cells of the coding sequence for the tox 176 attenuated diphtheria toxin A chain. *Mol. Cell. Biol.* **7,** 1576–1579 (1987).
21. Wee, R., Castrucci, A. M., Provencio, I., Gan, L. & Van Gelder, R. N. Loss of photic entrainment and altered free-running circadian rhythms in *math5*$^{-/-}$ mice. *J. Neurosci.* **22,** 10427–10433 (2002).
22. Gooley, J. J., Lu, J., Chou, T. C., Scammell, T. E. & Saper, C. B. Melanopsin in cells of origin of the retinohypothalamic tract. *Nature Neurosci.* **4,** 1165 (2001).
23. Barnard, A. R., Hattar, S., Hankins, M. W. & Lucas, R. J. Melanopsin regulates visual processing in the mouse retina. *Curr. Biol.* **16,** 389–395 (2006).
24. Iwakabe, H., Katsuura, G., Ishibashi, C. & Nakanishi, S. Impairment of pupillary responses and optokinetic nystagmus in the mGluR6-deficient mouse. *Neuropharmacology* **36,** 135–143 (1997).
25. Prusky, G. T., Alam, N. M., Beekman, S. & Douglas, R. M. Rapid quantification of adult and developing mouse spatial vision using a virtual optomotor system. *Invest. Ophthalmol. Vis. Sci.* **45,** 4611–4616 (2004).
26. Vorhees, C. V. & Williams, M. T. Morris water maze: procedures for assessing spatial and related forms of learning and memory. *Nature Protocols* **1,** 848–858 (2006).

Supplementary Information is linked to the online version of the paper at www.nature.com/nature.

Acknowledgements We thank J. Mackes and G. Harrison for help in genotyping the animals; R. Kuruvilla, M. Van Doren, B. Wendland, M. Halpern, M. Caterina, C.-Y. Su, J. Bradley and laboratory members in the Biology Department at the Johns Hopkins University for scientific discussions and comments on the manuscript. This work was supported by grants from the National Institutes of Health (to S. Hattar and K.-W.Y.), the Biotechnology and Biological Sciences Research Council (to R.J.L.) and the David and Lucile Packard and Alfred P. Sloan Foundations (to S. Hattar).

Author Contributions A.D.G. and S. Hattar wrote the paper. J.L.E., R.J.L., D.M.B. and T.C.B. gave helpful comments on the manuscript. A.D.G., J.L.E. and C.M.A. in S. Hattar's laboratory performed all the behavioural studies on the *aDTA* homozygous animals, as well as the X-gal staining of the *Opn4*$^{aDTA/tau\text{-}LacZ}$ and *Opn4*$^{tau\text{-}LacZ/+}$ animals, the morphology of the retina, the cholera toxin injections, the water maze and the optomotor studies. D.M.B. helped in analysing the brains of the *Opn4*$^{aDTA/tau\text{-}lacZ}$ and the cholera-toxin-injected animals. G.S.L. and A.R.B. in R.J.L.'s laboratory conducted all the behavioural studies on the *aDTA* heterozygous animals, and the electroretinogram studies. T.C.B. provided the construct and suggestions for the *aDTA* targeting strategy. H.C. made the optokinetic nystagmus recordings. H.-W.L. in K.-W.Y.'s laboratory performed the melanopsin immunostaining on *aDTA* heterozygous mice. Animals were first conceived in K.-W.Y.'s laboratory and produced by S. Hattar and S. Haq to the chimeric stage. Germline transmission was obtained independently in the laboratories of S. Hattar (with help from H.Z.) and K.-W.Y. All other authors helped in the planning, technical support and discussions of experiments.

Author Information Reprints and permissions information is available at www.nature.com/reprints. Correspondence and requests for materials should be addressed to S. Hattar (shattar@jhu.edu) or R.J.L. (robert.lucas@manchester.ac.uk).

METHODS

aDTA mice. Using the homologous arms that we used previously[3], we targeted the *aDTA* gene to the melanopsin locus. The targeting construct contained the diphtheria toxin A subunit and the neomycin resistance genes. The construct was flanked by 4.4 kilobases (kb) 5′ of the ATG site of the mouse melanopsin gene, and a 1.6-kb fragment containing 654 base pairs (bp) of exon 9 plus a 946-bp 3′ untranslated region. After electroporation of the linearized construct into 129.1 mouse strain embryonic stem cells and drug selection (400 μg ml^{-1} G418), one positive embryonic stem clone was injected into C57BL/6 blastocysts. Chimaeric animals were mated to C57BL/6 mice to produce heterozygous animals.

Immunostaining. Whole retinas from *Opn4*$^{aDTA/+}$ and wild-type animals, fixed in 70% ethanol, were immunostained with the C terminus melanopsin antibody (1:500 dilution). Fluorescently conjugated secondary antibody (Alexa Fluor 488 goat anti-rabbit IgG (1:1,000 dilution; Molecular Probes) was applied for 1–3 h.

Staining with X-gal. Animals anaesthetized by intraperitoneal injection of Avertin (20 ml kg^{-1}) were perfused intracardially with 4% paraformaldehyde, and brains and eyes were isolated. Eye-cups or brain sections (50 μm) were first incubated in buffer B (100 mM phosphate buffer at pH 7.4, 2 mM $MgCl_2$, 0.01% sodium deoxycholate, 0.02% IGEPAL) then stained for 3 days in buffer B plus 5 mM potassium ferricyanide, 5 mM potassium ferrocyanide and 1 mg ml^{-1} X-gal.

Cholera toxin injections in the eye. Mice were anaesthetized with Ketamine (80 mg kg^{-1})/Xylazine (8 mg kg^{-1}). Eyes were injected intravitreally with 2 μl of cholera toxin B subunit conjugated with Alexa Fluor 488 or Alexa Fluor 555 (Invitrogen). Three days after injection, brains were isolated and sectioned.

Electroretinograms. Animals maintained under 12:12 light/dark cycles for three days were used to collect data within the light phase (after 50 min of dark adaptation). The electroretinogram set-up was similar to that used previously[23]. Mydriatics (1% tropicamide and 2.5% phenylephrine) and hypromellose solution (0.3%) were used to dilate the pupil and retain corneal moisture in anaesthetized mice. A signal conditioner (Model 1902 Mark III; Cambridge Electronic Design) differentially amplified (×3,000) and filtered (bandpass filter cutoff 0.5–200 Hz) the signal before it was digitized (Model 1401 digitizer; Cambridge Electronic Design) and recorded (sampling rate 10 kHz) by means of Signal 2.15 software (Cambridge Electronic Design).

White light (10 ms in duration) was provided by a xenon arc source (Cairn Research). Neutral density filters (Edmund Optics) were used (unattenuated intensity 320 μW cm^{-2} at the cornea). For scotopic recordings, flashes were administered in the dark and testing began with the dimmest stimulus. Depending on the intensity, stimuli were presented at a rate of 0.5–0.2 Hz, and 6–20 repetitions were collected and averaged. Photopic electroretinograms were recorded by presentation of an unattenuated light (20 stimuli presented at a rate of 1 Hz) against blue-filtered (Grass blue filter; Astro-Med) rod-saturating background light (160 μW cm^{-2}).

Optokinetic nystagmus responses. A mouse stabilized with a head post was placed into an acrylic holder in a 12-inch diameter drum. Computer-generated stimuli were projected down onto the drum walls. Black and white stripes 4° in width were rotated at 5° s^{-1}. Eye movements of mice were captured with an infrared video system (ISCAN). The fast saccade components were counted in 30-s bins with an algorithm that evaluated the high-velocity eye movements that followed a low-velocity movement in the opposite direction.

Visual acuity. A virtual cylinder OptoMotry (Cerebral Mechanics) was used to determine visual acuity by measuring the image-tracking reflex of mice[25]. A sine-wave grating was projected on the screen rotating in a virtual cylinder. The animal was assessed for a tracking response on stimulation for about 5 s. All acuity thresholds were determined by using the staircase method with 100% contrast.

Morris water maze. To assess the ability of mice to detect a visual cue, we trained the animals to find a platform marked by a 10-cm tall, high-contrast visual cue under bright light (500 lx) in an 85-cm pool. On day 1, mice were trained with four trials 15 min apart. On the following day, latency to find the island was recorded first with the cue and then without it.

PLR. All animals were dark-adapted for at least 1 h, and the eye of each animal receiving the photic stimulus was treated with 0.1% atropine before the start of recording. Measurements were restricted to the middle of the subjective day (CT4–8). One eye of each mouse was digitally captured at a frequency of one image per second for 63 s with a charge-coupled-device camera. The light stimuli (xenon arc light source) consisted of a 60-s pulse at an intensity of 3.8 mW cm^{-2} or 1.8 μW cm^{-2} of white light.

For the *Opn4*$^{aDTA/aDTA}$ experiments, the eye receiving the photic stimulus was treated with 1% atropine. While one eye received light stimulation from a 470-nm light-emitting-diode light source (E27-B24; 161 μW cm^{-2}; Super Bright LEDs), a digital camcorder (DCRHC96; Sony) was used to record from the other eye (for 30 s) at 30 frames s^{-1} under a 940-nm light (LDP). The digital video recoding was deconstructed to individual frames with Blaze MediaPro software (Mystik Media). The percentage pupil constriction was calculated as the percentage of pupil area at 30 s after initiation of the stimulus (steady state) relative to the dilated pupil size.

Wheel running activity. Mice were placed in cages with a 4.5-inch running wheel, and their activity was monitored with VitalView software (Mini Mitter). The period was calculated with ClockLab (Actimetrics). For phase-shifting experiments, each animal was exposed to a light pulse (1,500 lx; CT16) for 15 min. After 41 days of constant dark, mice were re-entrained to 12:12 light/dark cycles for 19 days. Animals were then exposed to two jet-lag models: 16 days of a 6-h advance followed by 32 days of a 6-h delay. During the last two weeks of this treatment the animals were tested for PLR. Animals were then exposed to constant light for three weeks followed by ultradian 3.5:3.5 light/dark cycles.